

Muon spin relaxation and magnetic susceptibility studies of the effects of nonmagnetic impurities on the Cu spin dynamics and superconductivity in $\text{La}_{2-x}\text{Sr}_x\text{Cu}_{1-y}\text{Zn}_y\text{O}_4$ around $x=0.115$

著者	小池 洋二
journal or publication title	Physical review. B
volume	69
number	18
page range	184507-1-184507-10
year	2004
URL	http://hdl.handle.net/10097/35343

doi: 10.1103/PhysRevB.69.184507

Muon spin relaxation and magnetic susceptibility studies of the effects of nonmagnetic impurities on the Cu spin dynamics and superconductivity in $\text{La}_{2-x}\text{Sr}_x\text{Cu}_{1-y}\text{Zn}_y\text{O}_4$ around $x=0.115$

T. Adachi, S. Yairi, K. Takahashi, and Y. Koike

Department of Applied Physics, Graduate School of Engineering, Tohoku University, Aoba-yama 05, Aoba-ku, Sendai 980-8579, Japan

I. Watanabe

Muon Science Laboratory, RIKEN (The Institute of Physical and Chemical Research), 2-1 Hirosawa, Wako 351-0198, Japan

K. Nagamine

Meson Science Laboratory, Institute of Materials Structure Science, High Energy Accelerator Research Organization, 1-1 Oho, Tsukuba 305-0801, Japan

(Received 8 June 2003; revised manuscript received 18 November 2003; published 21 May 2004)

Zero-field muon-spin-relaxation (μSR) and magnetic-susceptibility measurements have been carried out in $\text{La}_{2-x}\text{Sr}_x\text{Cu}_{1-y}\text{Zn}_y\text{O}_4$ with $x=0.10, 0.115,$ and 0.13 changing the Zn concentration y finely up to 0.10 , with the aim to clarify effects of the nonmagnetic impurity Zn on the Cu-spin dynamics and superconductivity. The μSR measurements have revealed that, in each x , a magnetic order of Cu spins is observed at $y\sim 0.0075$, while it disappears and Cu spins turn into a fast fluctuating state for $y>0.03$. From the magnetic-susceptibility measurements, on the other hand, it has been found that the volume fraction of the superconducting state rapidly decreases through the slight doping of Zn and that its y dependence corresponds to the y dependence of the volume fraction of the fast fluctuating region of Cu spins estimated from the μSR results. Both the rapid decrease of the volume fraction of the superconducting state and the formation of the magnetic order through the slight doping of Zn can be interpreted in terms of the development of the so-called “Swiss cheese” model. That is, it is concluded that Cu spins in a nonsuperconducting region around Zn exhibit slowingdown of the fluctuations or form an incoherent or coherent static magnetic order. Moreover, the formation of a nonsuperconducting region around Zn is considered to be due to the pinning of the dynamical spin correlation or dynamical stripe correlations.

DOI: 10.1103/PhysRevB.69.184507

PACS number(s): 74.72.Dn, 76.75.+i, 74.25.Ha, 74.62.Dh

I. INTRODUCTION

There have been a great number of studies of the effects of nonmagnetic impurities in the high- T_c superconductors in past years. It is well known that local magnetic moments due to Cu spins are induced by the nonmagnetic impurity Zn in the underdoped regime^{1,2} and that the superconductivity is strongly suppressed by Zn.^{3,4} Recently, from the scanning-tunneling-microscopy (STM) measurements in the Zn-substituted Bi-2212 system, it has been found that the density of states of quasiparticles increases around each Zn in the superconducting state, suggesting the local destruction of superconductivity.⁵

On the other hand, the effect of nonmagnetic impurities on the dynamical stripe correlations of spins and holes suggested from the neutron scattering measurements in $\text{La}_{1.6-x}\text{Nd}_{0.4}\text{Sr}_x\text{CuO}_4$ with $x=0.12,$ ^{6,7} has been another issue with rising interest. It has been proposed that the dynamical stripe correlations are pinned and stabilized not only by the characteristic structure (the tetragonal low-temperature structure in the La-214 system) but also by nonmagnetic impurities such as Zn. This pinning has been considered to cause the so-called 1/8 anomaly, namely, the conspicuous suppression of superconductivity at p (the hole concentration per Cu) $\sim 1/8$. In $\text{La}_{2-x}\text{Sr}_x\text{Cu}_{1-y}\text{Zn}_y\text{O}_4$ with $x=0.115,$ in fact, the superconductivity is dramatically suppressed through only 1% substitution of Zn for Cu.⁸ Detailed measurements of the thermoelectric power and Hall coefficient in

$\text{La}_{2-x}\text{Sr}_x\text{Cu}_{1-y}\text{Zn}_y\text{O}_4$ have suggested that the dynamical stripe correlations tend to be pinned and stabilized by a small amount of Zn, while the static stripe order is destroyed by a large amount of Zn.⁹⁻¹¹ Such a stripe-pinning model owing to a small amount of Zn is supported by the theoretical studies based upon the t - J model.^{12,13}

Muon-spin-relaxation (μSR) measurements have provided a crucial probe to study the magnetism of the 1/8 anomaly in the La-214 system.¹⁴⁻¹⁸ In $\text{La}_{2-x}\text{Ba}_x\text{CuO}_4$ with $x=0.125,$ for instance, muon-spin precession has been observed at low temperatures below ~ 30 K, corresponding to the formation of a magnetic order of Cu spins.¹⁵⁻¹⁷ Moreover, the μSR technique makes it possible to distinguish between magnetic and nonmagnetic regions. A μSR study focusing on the Zn effect has been reported by Nachumi *et al.* for $y\leq 0.01$ in $\text{La}_{2-x}\text{Sr}_x\text{Cu}_{1-y}\text{Zn}_y\text{O}_4$ with $x=0.15$ and 0.20 and for $y\leq 0.015$ in $\text{YBa}_2(\text{Cu}_{1-y}\text{Zn}_y)_3\text{O}_{6.63},$ where the so-called “Swiss cheese” model has been proposed.¹⁹ They have observed two kinds of signal due to magnetic and nonmagnetic regions in one sample in the transverse-field μSR measurements, so that they have speculated that each Zn introduced in the CuO_2 plane produces a nonsuperconducting region around itself like Swiss cheese. However, this model has given no information about the Cu-spin fluctuations.

In this paper, we investigate the Cu-spin dynamics from the zero-field (ZF) μSR measurements of the Zn-substituted

$\text{La}_{2-x}\text{Sr}_x\text{Cu}_{1-y}\text{Zn}_y\text{O}_4$ with $x=0.10, 0.115,$ and 0.13 changing y finely up to 0.10 . We aim at clarifying from the view point of the spin dynamics whether the pinning of the dynamical stripe correlations by Zn is observed or not. We evaluate the Zn-concentration dependence of the volume fractions of different states of Cu spins with very different fluctuation frequencies.^{20–23} We also investigate the Zn effect on the superconductivity from the magnetic-susceptibility measurements. We evaluate the Zn-concentration dependence of the volume fraction of the superconducting state. Then, in comparison between the volume fractions of different states of Cu spins and the volume fraction of the superconducting state, we aim at elucidating the relation between the Cu-spin dynamics and superconductivity.²³

II. EXPERIMENTAL DETAILS

Polycrystalline samples of $\text{La}_{2-x}\text{Sr}_x\text{Cu}_{1-y}\text{Zn}_y\text{O}_4$ with $x=0.10, 0.115, 0.13$ and $y=0, 0.0025, 0.005, 0.0075, 0.01, 0.02, 0.03, 0.05, 0.07, 0.10$ were prepared by the ordinary solid-state reaction method. Appropriate powders of dried $\text{La}_2\text{O}_3, \text{SrCO}_3, \text{CuO},$ and ZnO were mixed and prefired in air at 900°C for 12 h. The prefired materials were mixed and pelletized, followed by sintering in air at 1050°C for 24 h. Postannealing was performed in flowing oxygen gas at 500°C for 72 h in order to keep oxygen deficiencies to a minimum. All of the samples were checked by the powder x-ray diffraction measurements to be single phase. The electrical resistivity was also measured to check the quality of the samples.

The ZF- μSR measurements were performed at the RIKEN-RAL Muon Facility at the Rutherford-Appleton Laboratory in the UK, using a pulsed positive surface muon beam with an incident muon momentum of $27\text{ MeV}/c$. The asymmetry parameter $A(t)$ at a time t was given by $A(t) = \{F(t) - \alpha B(t)\} / \{F(t) + \alpha B(t)\}$, where $F(t)$ and $B(t)$ were total muon events of the forward and backward counters, which were aligned in the beam line, respectively. α is the calibration factor reflecting the relative counting efficiencies between the forward and backward counters. The μSR time spectrum, namely, the time evolution of $A(t)$ was measured down to 2 K to detect the appearance of a magnetic order.

Magnetic-susceptibility measurements were carried out down to 2 K using a standard SQUID magnetometer (Quantum Design, Model MPMS-XL5) in a magnetic field of 10 Oe on field cooling, in order to evaluate the volume fraction of the superconducting state. In the case that a nonsuperconducting region in a sample is surrounded by a superconducting region, in fact, the superconducting volume fraction should be estimated from the value of the magnetic susceptibility on field cooling rather than on zero-field cooling. Even on field cooling, the vortex pinning effect in the superconducting region must be taken into account to evaluate the volume fraction precisely, but the effect is negligible to evaluate the volume fraction roughly in $\text{La}_{2-x}\text{Sr}_x\text{CuO}_4$.^{24,25}

III. RESULTS

A. ZF- μSR

Figure 1 displays the ZF- μSR time spectra of $\text{La}_{2-x}\text{Sr}_x\text{Cu}_{1-y}\text{Zn}_y\text{O}_4$ with $x=0.10, 0.115, 0.13$ and $y=0-0.10$. At a high temperature of 15 K or 20 K, all the spectra show Gaussian-like depolarization due to the randomly oriented nuclear spins. Focusing on the spectra at 2 K, muon-spin precession is observed in the Zn-free sample with $x=0.115$. This is clearly seen in Fig. 2, indicating the formation of a long-range magnetic order of Cu spins at low temperatures. As seen in Fig. 1, the deviation of x from 0.115 in the Zn-free samples leads to the destabilization of the magnetic order. That is, no precession of muon spins is observed for $x=0.10$. Even fast depolarization of muon spins is not observed for $x=0.13$. These indicate that the magnetic order is most developed at $x=0.115$ where the superconductivity is most suppressed.^{14,18}

With increasing y , muon-spin precession is clearly observed at $y \sim 0.0075$ in each x . Since the precession pattern is almost identical with one another in each x for $y=0.02$ where the most coherent precession is observed among all y , as seen in Fig. 2, it appears that nearly the same magnetic order is formed at $y \sim 0.02$ in each x . For $y > 0.03$, on the other hand, the muon-spin precession disappears and almost no fast depolarization of muon spins is observed at $y=0.10$. These mean that the static magnetic order is destroyed and that Cu spins are fluctuating with shorter periods than the μSR time window ($10^{-6}-10^{-11}$ sec) at $y=0.10$.

In order to derive the detailed information about the Cu-spin dynamics from the μSR results, we attempt to analyze the time spectra with the following three-component function:

$$A(t) = A_0 e^{-\lambda_0 t} G_Z(\Delta, t) + A_1 e^{-\lambda_1 t} + A_2 e^{-\lambda_2 t} \cos(\omega t + \phi). \quad (1)$$

The first term represents the slowly depolarizing component in a region where the Cu spins are fluctuating fast beyond the μSR time window. A_0 and λ_0 are the initial asymmetry and depolarization rate of the slowly depolarizing component, respectively, and $G_Z(\Delta, t)$ is the static Kubo-Toyabe function with a half-width of Δ describing the distribution of the nuclear-dipole field at the muon site.²⁶ The second term represents the fast depolarizing component in a region where the Cu-spin fluctuations slow down and/or an incoherent magnetic order is formed. A_1 and λ_1 are the initial asymmetry and depolarization rate of the fast depolarizing component, respectively. The third term represents the muon-spin precession in a region where a coherent static magnetic order of Cu spins is formed. A_2 is the initial asymmetry. λ_2 , ω , and ϕ are the damping rate, frequency, and phase of the muon-spin precession, respectively. The time spectra are well fitted with Eq. (1), as shown by solid lines in Figs. 1 and 2.

Figure 3 shows the temperature dependence of A_0 obtained from the best fit using Eq. (1) for typical y values in $\text{La}_{2-x}\text{Sr}_x\text{Cu}_{1-y}\text{Zn}_y\text{O}_4$ with $x=0.10, 0.115,$ and 0.13 . The value of A_0 is normalized by its value at a high temperature

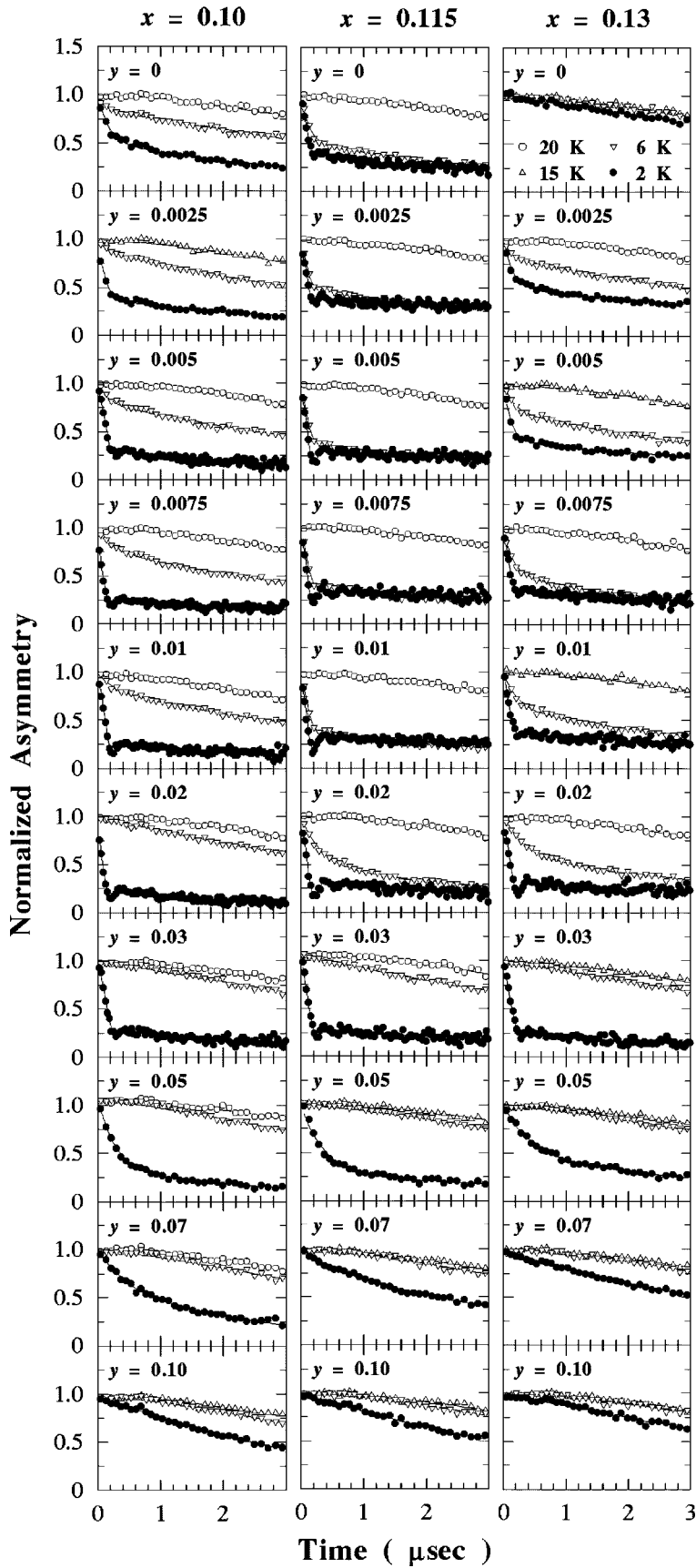


FIG. 1. ZF- μ SR time spectra of $\text{La}_{2-x}\text{Sr}_x\text{Cu}_{1-y}\text{Zn}_y\text{O}_4$ with $x=0.10, 0.115, 0.13$ and $y=0-0.10$ at various temperatures down to 2 K. Time spectra in the early time region from 0 to 3 μsec are displayed. Solid lines indicate the best-fit results using $A(t) = A_0 e^{-\lambda_0 t} G_Z(\Delta, t) + A_1 e^{-\lambda_1 t} + A_2 e^{-\lambda_2 t} \cos(\omega t + \phi)$.

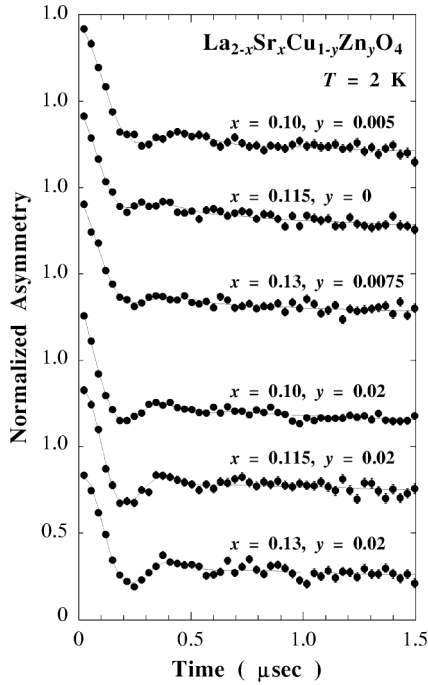


FIG. 2. ZF- μ SR time spectra at 2 K in the very early time region from 0 to 1.5 μ sec for $\text{La}_{2-x}\text{Sr}_x\text{Cu}_{1-y}\text{Zn}_y\text{O}_4$ with $x = 0.10, 0.115,$ and 0.13 . The y values shown in the upper three spectra correspond to the values where the muon-spin precession starts to be observed with increasing y , while those shown in the lower three spectra correspond to the values where the muon-spin precession is most clearly observed among all y in each x . Solid lines indicate the best-fit results using $A(t) = A_0 e^{-\lambda_0 t} G_Z(\Delta, t) + A_1 e^{-\lambda_1 t} + A_2 e^{-\lambda_2 t} \cos(\omega t + \phi)$.

of 15 K or 20 K. The temperature dependence of A_0 is often used as a probe of the magnetic transition, because it reflects the volume fraction of the nonmagnetic region.^{14,17,18} In fact, $A_0 = 1$ means that the spectrum is represented only with the first term of Eq. (1), indicating that all the Cu spins are fluctuating fast beyond the μ SR time window. On the contrary, $A_0 = 1/3$ indicates that all the Cu spins are nearly or completely ordered statically. As shown in Fig. 3, A_0 becomes almost 1/3 at 2 K for $y = 0.005\text{--}0.05$ in $x = 0.10$, $y = 0\text{--}0.05$ in $x = 0.115$, and $y = 0.01\text{--}0.03$ in $x = 0.13$, indicating the formation of the magnetic order. For the Zn-free samples with $x = 0.10$ and 0.115 and the 0.5% Zn-substituted sample with $x = 0.13$, the transition to the magnetically ordered state is rather broad, though the onset temperature T_N^{onset} defined as the temperature where A_0 starts to deviate from 1 with decreasing temperature, is higher than T_N^{onset} for the Zn-substituted samples with $x = 0.10$ and 0.115 and for the Zn-substituted samples with $x = 0.13$ and $y \geq 0.02$, respectively. With increasing y , the magnetic transition tends to be sharp. At $y = 0.10$, no decrease in A_0 from 1 is observed. The details of these behaviors depending on y are discussed in Sec. IV.

We estimate the magnetic transition temperature T_N^{mid} , defined as the midpoint of the change of the A_0 value from 1 to the minimum value $A_{0\text{min}}$ in each x .²⁷ Figure 4(a) shows the Zn-concentration dependence of T_N^{mid} for

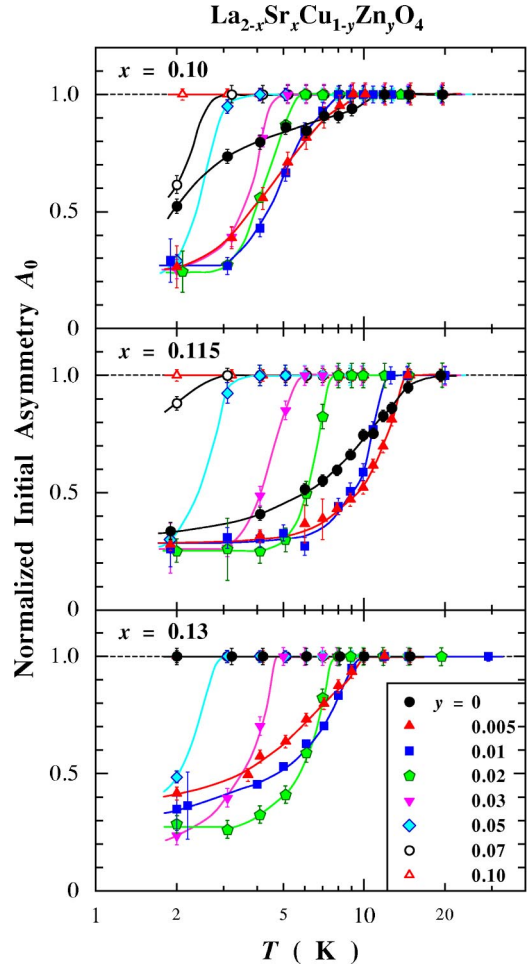


FIG. 3. (Color online) Temperature dependence of the initial asymmetry of the slowly depolarizing component A_0 , normalized by its value at a high temperature of 15 K or 20 K, for the typical y values in $\text{La}_{2-x}\text{Sr}_x\text{Cu}_{1-y}\text{Zn}_y\text{O}_4$ with $x = 0.10, 0.115,$ and 0.13 . Solid lines are to guide the reader's eye.

$\text{La}_{2-x}\text{Sr}_x\text{Cu}_{1-y}\text{Zn}_y\text{O}_4$ with $x = 0.10, 0.115,$ and 0.13 . For $x = 0.10$ and 0.115 , T_N^{mid} increases with increasing y and shows the maximum at $y \sim 0.0075$. In the case of $x = 0.13$, T_N^{mid} appears at $y = 0.0025$ and shows the maximum at $y \sim 0.01$. Above $y \sim 0.01$, on the other hand, T_N^{mid} decreases gradually with increasing y and finally disappears above $y \sim 0.05$ or 0.07 in each x . Figure 4(b) shows the Zn-concentration dependence of T_N^{onset} . The T_N^{onset} decreases almost monotonically with increasing y . These results indicate that the transition toward the formation of the magnetic order is rather broad at $y \sim 0$, while it becomes sharp through the introduction of Zn, as mentioned in the preceding paragraph.

Next, we estimate the volume fractions of the three different states of Cu spins in one sample related to the three terms in Eq. (1), respectively, using the best-fit values of A_0 , A_1 , and A_2 . As A_0 is not zero but $A_{0\text{min}}$ even in a completely magnetically ordered state, the volume fraction V_{A_0} of the region where the Cu spins are fluctuating fast beyond the μ SR time window (we call this region the A_0 region) is given by

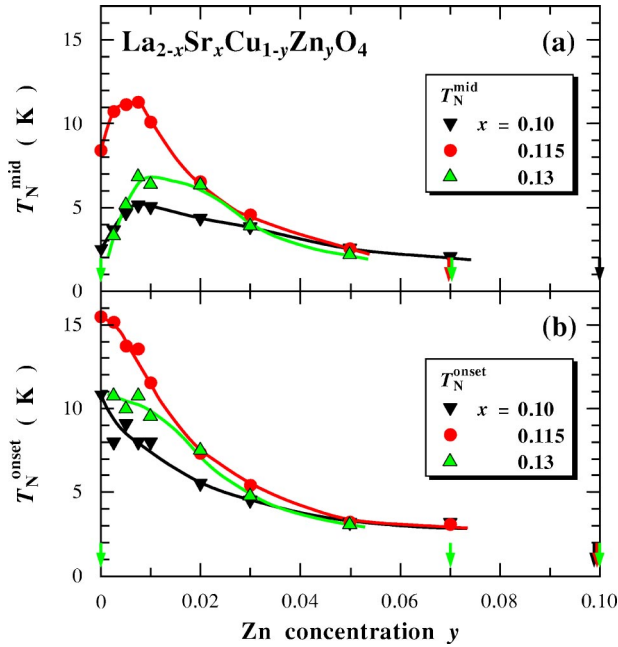


FIG. 4. (Color online) Zn-concentration dependence of (a) T_N^{mid} defined as the midpoint of the change of the A_0 value from 1 to $A_{0\text{min}}$ and (b) the onset temperature of the magnetic transition T_N^{onset} for $\text{La}_{2-x}\text{Sr}_x\text{Cu}_{1-y}\text{Zn}_y\text{O}_4$ with $x=0.10, 0.115,$ and 0.13 . Solid lines are to guide the reader's eye.

$$V_{A_0} = \frac{A_0 - A_{0\text{min}}}{(A_0 + A_1 + A_2) - A_{0\text{min}}}. \quad (2)$$

The volume fraction V_{A_1} of the region where the Cu-spin fluctuations slow down and/or an incoherent magnetic order is formed (the A_1 region) is given by²⁸

$$V_{A_1} = \frac{A_1}{(A_0 + A_1 + A_2) - A_{0\text{min}}}. \quad (3)$$

The volume fraction V_{A_2} of the region where a coherent static magnetic order is formed (the A_2 region) is given by

$$V_{A_2} = \frac{A_2}{(A_0 + A_1 + A_2) - A_{0\text{min}}}. \quad (4)$$

Figure 5 displays the Zn-concentration dependence of the volume fraction V_{A_0} , V_{A_1} , and V_{A_2} at 2 K for $\text{La}_{2-x}\text{Sr}_x\text{Cu}_{1-y}\text{Zn}_y\text{O}_4$ with $x=0.10, 0.115,$ and 0.13 . For $x=0.13$, V_{A_0} is 100% at $y=0$, indicating that all the Cu spins are fluctuating at high frequencies. With increasing y , V_{A_0} rapidly decreases and V_{A_1} increases complementarily, indicating the slowingdown of the Cu-spin fluctuations and/or the formation of an incoherent magnetic order. In fact, V_{A_2} increases instead of V_{A_1} for $y>0.005$. At $y=0.02$, V_{A_0} becomes zero and almost all the Cu spins become static and are magnetically ordered. On the other hand, V_{A_2} decreases with increasing y for $y>0.02$, meaning the destabilization of the magnetic order. At $y=0.10$, V_{A_0} again becomes 100%, indicating that all the Cu spins are fluctuating at high frequencies again.

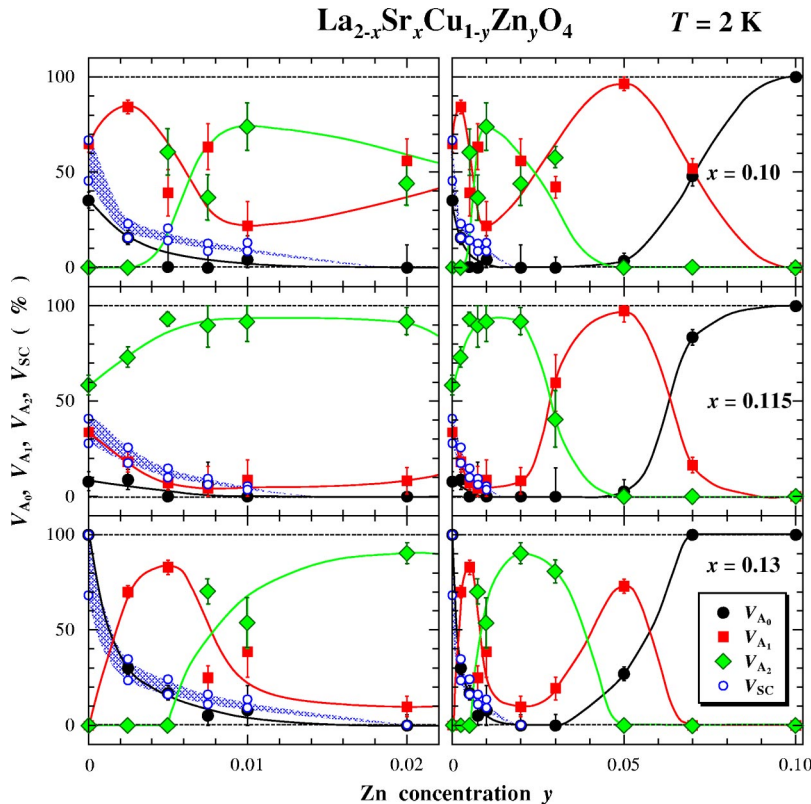


FIG. 5. (Color online) Dependence on y of V_{A_0} (black circles), V_{A_1} (red squares), and V_{A_2} (green diamonds) estimated from the μSR measurements at 2 K in $\text{La}_{2-x}\text{Sr}_x\text{Cu}_{1-y}\text{Zn}_y\text{O}_4$ with $x=0.10, 0.115,$ and 0.13 . Dependence on y of V_{SC} (blue shadow area surrounded by blue open circles) estimated from the magnetic-susceptibility measurements at 2 K is also plotted. V_{A_0} : Volume fraction of the region where the Cu spins are fluctuating fast beyond the μSR time window. V_{A_1} : Volume fraction of the region where the Cu-spin fluctuation slow down and/or an incoherent magnetic order is formed. V_{A_2} : Volume fraction of the region where a coherent static magnetic order is formed. V_{SC} : Volume fraction of the superconducting region. Note that left panels are magnification of right panels from $y=0$ to $y=0.022$. Solid lines are to guide the reader's eye.

As for $x=0.10$ and 0.115 , almost similar Zn-concentration dependence of the volume fractions of the respective Cu-spin states are obtained, but the important difference among $x=0.10$, 0.115 , and 0.13 is in the Cu-spin state of the Zn-free sample. For $x=0.115$, V_{A_0} is less than 10%, while V_{A_2} is more than 50%. For $x=0.10$, on the other hand, V_{A_1} is more than 60%, while V_{A_2} is zero. These indicate that the magnetic order is most developed at $x=0.115$ in the Zn-free samples and is suddenly destabilized with the deviation of x from 0.115 .^{14,18} These results also give two important features; (i) the fast fluctuating region of Cu spins is rapidly diminished by the introduction of a small amount of Zn, and (ii) the slowly fluctuating and/or incoherent magnetically ordered region of Cu spins are replaced by a coherent magnetically ordered one for $y>0.005$. These behaviors are discussed in detail in Sec. IV.

B. Magnetic susceptibility

Figure 6 shows the temperature dependence of the magnetic susceptibility χ for $\text{La}_{2-x}\text{Sr}_x\text{Cu}_{1-y}\text{Zn}_y\text{O}_4$ with $x=0.10$, 0.115 , 0.13 and $y\leq 0.02$. In comparison between the absolute values of χ at 2 K $|\chi_{2\text{K}}|$ of the Zn-free samples with $x=0.10$, 0.115 , and 0.13 , $|\chi_{2\text{K}}|$ in $x=0.115$ is less than half of that in $x=0.13$. This means that the volume fraction of the superconducting state for $x=0.115$ is markedly suppressed even in the Zn-free sample. For $x=0.13$, on the other hand, $|\chi_{2\text{K}}|$ dramatically decreases through only 0.25% substitution of Zn. With increasing y from $y=0.0025$, $|\chi_{2\text{K}}|$ decreases gradually and is almost zero at $y=0.02$. This peculiar behavior of the decrease of $|\chi_{2\text{K}}|$ with increasing y suggests that the volume fraction of the superconducting state does not decrease linearly but is strongly suppressed by a very small amount of Zn. It is noted that the y dependence

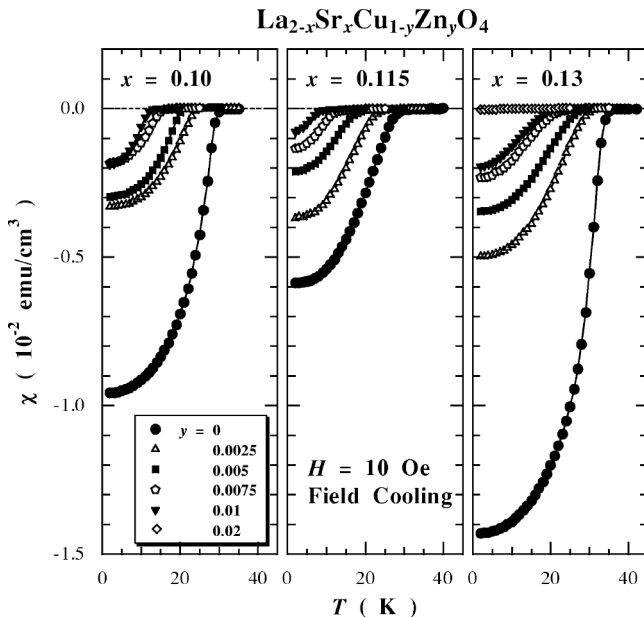


FIG. 6. Temperature dependence of the magnetic susceptibility χ of $\text{La}_{2-x}\text{Sr}_x\text{Cu}_{1-y}\text{Zn}_y\text{O}_4$ with $x=0.10$, 0.115 , and 0.13 in a magnetic field of 10 Oe on field cooling.

of $|\chi_{2\text{K}}|$ for $y\geq 0.0025$ in each x is roughly similar to one another, suggesting that the Zn-substituted states for $y\geq 0.0025$ are not so dependent on x .

We estimate the volume fraction of the superconducting state V_{SC} concretely from the value of $|\chi_{2\text{K}}|$. The value of $|\chi_{2\text{K}}|$ corresponding to 100% of V_{SC} is hard to be determined exactly. Thus, we choose two values, namely, the values of $|\chi_{2\text{K}}|$ of the Zn-free sample with $x=0.13$ and of the optimally doped Zn-free sample with $x=0.15$ as corresponding to 100% of V_{SC} .²⁴ Then, V_{SC} is estimated as the value of $|\chi_{2\text{K}}|$ in each x and y divided by that of the Zn-free sample with $x=0.13$ or 0.15 , as shown by blue open circles in Fig. 5. The true y dependence of V_{SC} must be located in the shadow area surrounded by the blue open circles. It is found that the y dependence of V_{SC} is analogous to that of V_{A_0} . Especially for $x=0.13$, the y dependence of V_{SC} is in good agreement with that of V_{A_0} . This gives an important information beyond the ‘‘Swiss cheese’’ model. That is, the superconductivity is realized in the region where Cu spins fluctuate fast beyond the μSR time window. In other words, Cu spins in a nonsuperconducting region around Zn exhibit slowingdown of the fluctuations or form an incoherent or coherent static order.

IV. DISCUSSION

First, we discuss the Zn-concentration dependence of V_{A_0} , V_{A_1} , V_{A_2} , and V_{SC} . Figure 7 displays schematic pictures of the spatial distribution of A_0 , A_1 , and A_2 regions with different Cu-spin states at 2 K for typical y values in $\text{La}_{2-x}\text{Sr}_x\text{Cu}_{1-y}\text{Zn}_y\text{O}_4$ with $x=0.13$, on the assumption that the magnetic order develops around each Zn for lightly Zn substituted samples.²⁹ This assumption has not yet been confirmed directly but is reasonable, referring to the result of the STM measurements in the Zn-substituted Bi-2212 system.⁵ Sizes of the circles are calculated from the ratio of V_{A_0} : V_{A_1} : V_{A_2} in each y . Through only 0.25% substitution of Zn for Cu, an A_1 region, namely, a slowly fluctuating and/or incoherent magnetically ordered region of Cu spins is formed with ξ_{ab} , defined as the radius of A_1 region at 2 K, ~ 36 Å around each Zn in the A_0 region, namely, in the fast fluctuating sea of Cu spins.³⁰ It is found that a large part of the CuO_2 plane is covered with A_1 regions so that V_{SC} in good correspondence to V_{A_0} is strongly diminished. Comparing ξ_{ab} with a mean distance between Zn atoms $R_{\text{Zn-Zn}}\sim 76$ Å at $y=0.0025$, A_1 regions are averagely considered not to overlap one another. With increasing y , A_1 regions overlap one another at $y=0.005$, leading to the development of A_2 regions, namely, coherent magnetically ordered regions. In fact, A_0 regions almost disappear at $y=0.0075$ and alternatively A_2 regions are formed around Zn. Although plural patterns of the spatial distribution of A_2 regions are possible, the pattern where A_2 regions develop around Zn is shown in Fig. 7. When y reaches 0.02, A_2 regions cover the almost whole CuO_2 plane, leading to the formation of a nearly coherent magnetic order. With increasing y from $y=0.02$, A_2 regions decrease. They completely disappear at $y=0.05$ and alterna-

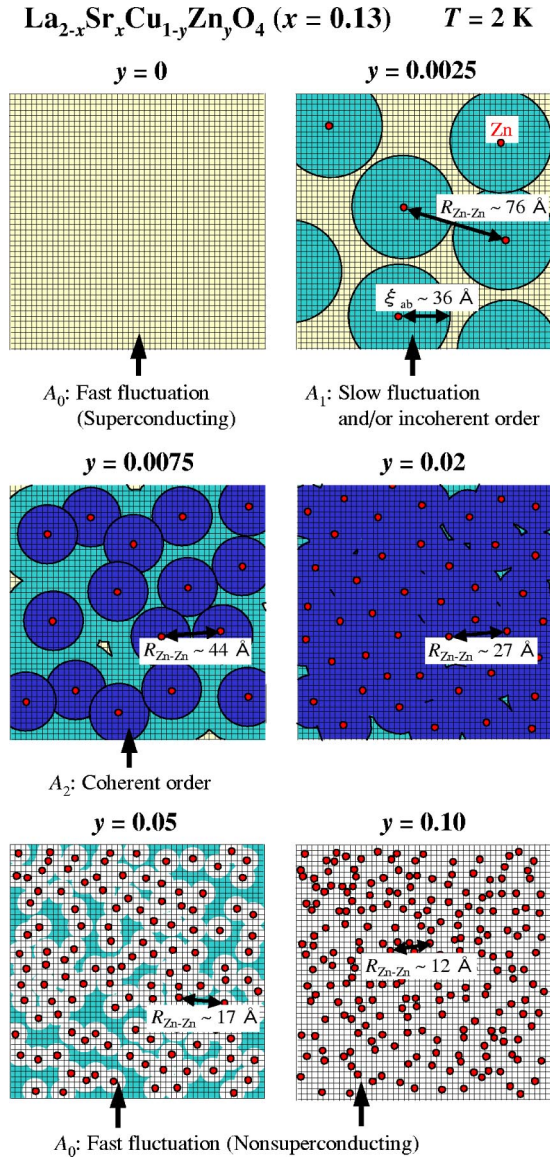


FIG. 7. (Color online) Schematic pictures of the spatial distribution of the different Cu-spin states in the CuO_2 plane, corresponding to A_0 , A_1 , and A_2 , at 2 K for typical y values in $\text{La}_{2-x}\text{Sr}_x\text{Cu}_{1-y}\text{Zn}_y\text{O}_4$ with $x=0.13$. Each crossing point of the grid pattern represents the Cu site. Zn atoms are randomly distributed in the CuO_2 plane. Sizes of the circles are calculated from the ratio of $V_{A_0} : V_{A_1} : V_{A_2}$ in each y . ξ_{ab} indicates the radius of the A_1 region around each Zn. $R_{\text{Zn-Zn}}$ indicates a mean distance between Zn atoms.

tively A_0 regions reappear. Here, reappeared A_0 regions are nonsuperconducting and considered to be formed around each Zn as shown in Fig. 7, because a large amount of nonmagnetic Zn destroys the magnetic order of Cu spins. At $y = 0.10$, the nonsuperconducting A_0 regions cover the whole CuO_2 plane. These changes with increasing y suggest that the superconducting region competes with both the slowly fluctuating and magnetically ordered regions of Cu spins. As for the 0.25% Zn-substituted samples with $x=0.10$, 0.115, and 0.13, ξ_{ab} is not so different from one another but largest at $x=0.115$, as shown in Fig. 8. For $x=0.115$, moreover, A_2

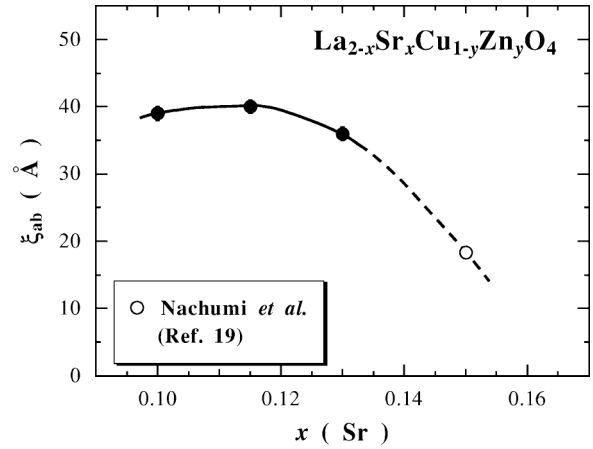


FIG. 8. Dependence on x of the radius ξ_{ab} of the A_1 region around each Zn, estimated from the ratio of $V_{A_0} : V_{A_1} : V_{A_2}$ at $y = 0.0025$, for $\text{La}_{2-x}\text{Sr}_x\text{Cu}_{1-y}\text{Zn}_y\text{O}_4$. The data of $x=0.15$ are from Ref. 19. The solid and dashed line is to guide the reader's eye.

regions are developed even for $y \leq 0.0025$, as shown in Fig. 5. These suggest that the magnetic order tends to develop especially at $x=0.115$.

Here, we discuss the Cu-spin state of the nonsuperconducting region around Zn. An analogous model on the Zn effect has been proposed by Nachumi *et al.*, which is known as the “Swiss cheese” model.¹⁹ In this model, it has been estimated that Zn destroys the superconductivity around itself with the radius $\xi_{ab} = 18.3 \text{ \AA}$ for $x=0.15$ in $\text{La}_{2-x}\text{Sr}_x\text{Cu}_{1-y}\text{Zn}_y\text{O}_4$. Our estimation of $\xi_{ab} \sim 40 \text{ \AA}$ for $x=0.115$ is more than twice as large as that for $x=0.15$, as shown in Fig. 8. One may easily guess that the difference in ξ_{ab} originates from that in the hole concentration. That is, more holes in $x=0.15$ than in $x=0.115$ are expected to disturb the formation of the static magnetic order. However, this may not be the case, because ξ_{ab} for $x=0.10$ is not larger than that for $x=0.115$. We speculate that the difference in ξ_{ab} is related to the spin-correlation length in the region where Zn destroys the superconductivity, because V_{SC} is analogous to V_{A_0} . Considering that the correlation length of the incommensurate dynamical spin correlation estimated from the inelastic neutron scattering measurements³¹ is larger for $x=0.12$ than for $x=0.15$, the large nonsuperconducting region induced by Zn is understood to be due to the large correlation length of the dynamical spin correlation. This means that the dynamical spin correlation or the dynamical stripe correlations tend to be pinned and stabilized by Zn. Furthermore, the overlap between the pinned regions leads to the formation of the static spin order. Although the spin state of the nonsuperconducting region around each Zn has not been clear in the “Swiss cheese” model, it is identified from our results that the nonsuperconducting region around each Zn corresponds to the statically ordered region pinned by Zn. This interpretation is regarded as a kind of development of the “Swiss cheese” model.

Comparison between the results of the recent neutron scattering measurements and the present μSR results is of much interest. In $\text{La}_{2-x}\text{Sr}_x\text{CuO}_4$ with $x=0.10$, Lake *et al.*³² have reported that the intensity of the incommensurate elas-

tic magnetic peaks around (π, π) in the reciprocal space observed in zero field³³ is enhanced by the application of magnetic field. In the Zn-substituted $\text{La}_{2-x}\text{Sr}_x\text{Cu}_{1-y}\text{Zn}_y\text{O}_4$ with $x=0.15$ where a gap opens below ~ 3.5 meV in the spin excitation spectrum,³⁴ it has been found by Kimura *et al.*³⁵ that Zn induces the so-called in-gap state in the spin gap, suggesting tendency toward the formation of a static spin order. These experimental results have been interpreted as induction of a local antiferromagnetic (AF) order inside the vortex core or around Zn. Moreover, the induced AF order turns out to have coherency between them with increasing magnetic field or Zn concentration, leading to the enhancement of the incommensurate magnetic peaks. Our interpretation of the present μSR results is quite similar with respect to the formation of a local magnetic order around Zn. That is, it is confirmed in Fig. 7 that the overlap between A_1 regions around Zn generates coherency between the Cu spins inside A_1 regions, leading to the formation of the coherent magnetic order. In the case of $x=0.115$ where the magnetic order is formed even in the Zn-free sample, the coherent magnetic order develops a little with increasing Zn concentration. This μSR result is quite consistent with a little enhancement of the incommensurate magnetic peaks induced by magnetic fields in the neutron scattering measurements in $\text{La}_{2-x}\text{Sr}_x\text{CuO}_4$ with $x=0.12$ by Katano *et al.*³⁶ In addition, it is noted that V_{A_0} is not zero in the Zn-free sample with $x=0.115$, implying that the incommensurate magnetic peaks observed from the elastic neutron scattering measurements in the Zn-free sample with $x\sim 0.115$ (Refs. 36–38) do not necessarily correspond to the magnetic order formed throughout the sample. These results support our speculation that the dynamical spin correlation or the dynamical stripe correlations tend to be pinned and stabilized around Zn.

Next, we discuss the peculiar dependence of the magnetic transition on the Zn concentration, as shown in Fig. 3. In the Zn-free or slightly Zn-substituted samples, the magnetic transition is rather broad, though T_N^{onset} is comparatively high. With increasing y , on the contrary, T_N^{onset} decreases as also shown in Fig. 4(b) and the transition tends to be sharp. This means that the fluctuation of the magnetic transition is large in the Zn-free or slightly Zn-substituted samples. In the moderately Zn-substituted samples, on the other hand, the fluctuation of the magnetic transition is comparatively small. It appears that Zn operates to pin the dynamical spin correlation or the dynamical stripe correlations so as to suppress the fluctuation of the magnetic transition, as suggested from our transport measurements.^{9–11} The decrease of T_N^{onset} with increasing y may be attributed to weakening of the spin correlation due to the spin-dilution effect of the nonmagnetic Zn.

As for the increase in T_N^{mid} with increasing y for $y < 0.01$, a qualitatively similar behavior has been observed in the three-dimensional (3D) antiferromagnetically ordered region ($x < 0.02$) of $\text{La}_{2-x}\text{Sr}_x\text{Cu}_{1-y}\text{Zn}_y\text{O}_4$ by Hücker *et al.*³⁹ They have insisted that the localization of holes around the substituted Zn restores the AF correlation between Cu spins, resulting in the increase in T_N with increasing y . This scenario may be substantially suitable but is a little different

from the case of $x\sim 0.115$. Considering that the dynamical stripe correlations of spins and holes exist at $x\sim 0.115$, it is likely that the dynamical stripe correlations are pinned and stabilized by Zn, leading to both the localization of holes in the one-dimensional charge domain and the increase in T_N^{mid} .

Finally, we argue the Cu-spin state in the heavily Zn-substituted samples with $y > 0.02$. The V_{A_2} decreases gradually with increasing y for $y > 0.02$ and the muon-spin precession is no longer observed at $y > 0.03$ in each x , meaning that the magnetic order is destabilized with increasing Zn concentration for $y > 0.02$. At $y=0.10$, almost no fast depolarization of muon spins is observed, indicating that even a spin-glass state is not realized but the spin correlation becomes weak through the introduction of a large amount of Zn due to the spin-dilution effect of the nonmagnetic Zn.³⁹ Furthermore, considering that the 3D AF order survives through the introduction of Zn up to $y\sim 0.4$ in the Zn-substituted $\text{La}_2\text{Cu}_{1-y}\text{Zn}_y\text{O}_4$,⁴⁰ the destruction of the magnetic order through only the 5–7% substitution of Zn for $x\sim 0.115$ may be attributed to the mobile holes released from the possible stripe order.

In addition, it is worthwhile noting that, at $y\geq 0.07$ in $x=0.13$, V_{A_0} is 100% but superconductivity does not reappear. In the Zn-free sample with $x=0.13$, on the other hand, V_{A_0} is 100% and superconductivity takes place. Simply thinking, the 7% Zn substitution causes scattering of holes so frequently that holes tend to be localized, resulting in the destruction of the superconductivity as in the case of conventional superconductors. From the resistivity measurements, however, the value of the resistivity in the normal state at 50 K for the 7% Zn-substituted sample with $x=0.13$ is only about six times as large as that for the Zn-free sample with $x=0.13$ and as small as that for the Zn-free sample with $x=0.06$ where superconductivity appears at low temperatures.²⁴ Therefore, this may suggest that the dynamical spin correlation or dynamical stripe correlations are essential to the appearance of the high- T_c superconductivity.

V. SUMMARY

We have investigated effects of the nonmagnetic impurity Zn on the Cu-spin dynamics and superconductivity from the ZF- μSR and magnetic-susceptibility measurements in $\text{La}_{2-x}\text{Sr}_x\text{Cu}_{1-y}\text{Zn}_y\text{O}_4$ with $x=0.10, 0.115$, and 0.13 changing y finely up to 0.10 . The μSR measurements have revealed that, in each x , a magnetic order of Cu spins is observed at $y\sim 0.0075$, while it disappears and Cu spins turn into a fast fluctuating state for $y > 0.03$. It has been found that all the μSR spectra can be represented by the three-component function with different frequencies of the Cu-spin fluctuations. From the magnetic-susceptibility measurements, on the other hand, it has been found that the volume fraction of the superconducting state rapidly decreases through the slight doping of Zn and that its y dependence corresponds to the y dependence of the volume fraction of the fast fluctuating region of Cu spins estimated from the μSR results. From these results, it has been concluded that the nonsuperconducting region induced around Zn corresponds to the region where the Cu-spin fluctuations slow

down. In other words, it has been concluded that both the slowly fluctuating region of Cu spins and the magnetically ordered region compete with the superconductivity. Our results have been interpreted in terms of the development of the “Swiss cheese” model. That is, it is considered that Zn pins the dynamical spin correlation or dynamical stripe correlations and hence destroys the superconductivity around itself.

ACKNOWLEDGMENTS

We would like to thank Prof. Y.J. Uemura and Dr. H. Kimura for fruitful discussions. This work was supported by a Grant-in-Aid for Scientific Research from the Ministry of Education, Science, Sports, Culture, and Technology, Japan, and also by CREST of Japan Science and Technology Corporation.

- ¹A.V. Mahajan, H. Alloul, G. Collin, and J.F. Marucco, *Phys. Rev. Lett.* **72**, 3100 (1994).
- ²G. Xiao, M.Z. Cieplak, J.Q. Xiao, and C.L. Chien, *Phys. Rev. B* **42**, 8752 (1990).
- ³Y. Maeno and T. Fujita, *Physica C* **153-155**, 1105 (1988).
- ⁴Y. Koike, N. Watanabe, T. Noji, and Y. Saito, *Solid State Commun.* **78**, 511 (1991).
- ⁵S.H. Pan, E.W. Hudson, K.M. Lang, H. Eisaki, S. Uchida, and J.C. Davis, *Nature (London)* **403**, 746 (2000).
- ⁶J.M. Tranquada, B.J. Sternlieb, J.D. Axe, Y. Nakamura, and S. Uchida, *Nature (London)* **375**, 561 (1995).
- ⁷J.M. Tranquada, J.D. Axe, N. Ichikawa, Y. Nakamura, S. Uchida, and B. Nachumi, *Phys. Rev. B* **54**, 7489 (1996).
- ⁸Y. Koike, A. Kobayashi, T. Kawaguchi, M. Kato, T. Noji, Y. Ono, T. Hikita, and Y. Saito, *Solid State Commun.* **82**, 889 (1992).
- ⁹Y. Koike, S. Takeuchi, H. Sato, Y. Hama, M. Kato, Y. Ono, and S. Katano, *J. Low Temp. Phys.* **105**, 317 (1996).
- ¹⁰Y. Koike, S. Takeuchi, Y. Hama, H. Sato, T. Adachi, and M. Kato, *Physica C* **282-287**, 1233 (1997).
- ¹¹T. Adachi, T. Noji, H. Sato, Y. Koike, T. Nishizaki, and N. Kobayashi, *J. Low Temp. Phys.* **117**, 1151 (1999).
- ¹²T. Tohyama, M. Takahashi, and S. Maekawa, *Physica C* **357-360**, 93 (2001).
- ¹³C. Morais Smith, A.H. Castro Neto, and A.V. Balatsky, *Phys. Rev. Lett.* **87**, 177010 (2001).
- ¹⁴E. Torikai, I. Tanaka, H. Kojima, K. Kitazawa, and K. Nagamine, *Hyperfine Interact.* **63**, 271 (1990).
- ¹⁵K. Kumagai, I. Watanabe, K. Kawano, H. Matoba, K. Nishiyama, K. Nagamine, N. Wada, M. Okaji, and K. Nara, *Physica C* **185-189**, 913 (1991).
- ¹⁶G.M. Luke, L.P. Le, B.J. Sternlieb, W.D. Wu, Y.J. Uemura, J.H. Brewer, T.M. Riseman, S. Ishibashi, and S. Uchida, *Physica C* **185-189**, 1175 (1991).
- ¹⁷I. Watanabe, K. Kawano, K. Kumagai, K. Nishiyama, and K. Nagamine, *J. Phys. Soc. Jpn.* **61**, 3058 (1992).
- ¹⁸I. Watanabe, K. Nishiyama, K. Nagamine, K. Kawano, and K. Kumagai, *Hyperfine Interact.* **86**, 603 (1994).
- ¹⁹B. Nachumi, A. Keren, K. Kojima, M. Larkin, G.M. Luke, J. Merrin, O. Tchernyshöv, Y.J. Uemura, N. Ichikawa, M. Goto, and S. Uchida, *Phys. Rev. Lett.* **77**, 5421 (1996).
- ²⁰I. Watanabe, T. Adachi, K. Takahashi, S. Yairi, Y. Koike, and K. Nagamine, *J. Phys. Chem. Solids* **63**, 1093 (2002).
- ²¹I. Watanabe, T. Adachi, K. Takahashi, S. Yairi, Y. Koike, and K. Nagamine, *Phys. Rev. B* **65**, 180516(R) (2002).
- ²²I. Watanabe, T. Adachi, S. Yairi, Y. Koike, and K. Nagamine, *Physica B* **326**, 305 (2003).
- ²³T. Adachi, I. Watanabe, S. Yairi, K. Takahashi, Y. Koike, and K. Nagamine, *J. Low Temp. Phys.* **131**, 843 (2003).
- ²⁴S. Yairi, T. Adachi, and Y. Koike (unpublished).
- ²⁵T. Nagano, Y. Tomioka, Y. Nakayama, K. Kishio, and K. Kitazawa, *Phys. Rev. B* **48**, 9689 (1993).
- ²⁶Y.J. Uemura, T. Yamazaki, D.R. Harshman, M. Senba, and E.J. Ansaldo, *Phys. Rev. B* **31**, 546 (1985).
- ²⁷In the ideal case, $A_0 = 1/3$ in a magnetically ordered state. In some case, however, A_0 becomes smaller than $1/3$ even in the ordered state as seen in Fig. 3. Therefore, we have decided that A_0 becomes $A_{0\min}$, defined as the mean value among A_0 where the magnetic order is formed at 2 K, in the magnetically ordered state for each x and defined T_N^{mid} as the midpoint temperature in the change of A_0 .
- ²⁸In this calculation, we have assumed that all the Cu spins in the A_1 region contribute to the formation of an incoherent magnetic order. In the case that all the Cu spins in the A_1 region fluctuate slowly, the value of V_{A_1} slightly decreases as mentioned in Sec. IV. However, the use of Eq. (3) for the estimation of V_{A_1} is considered to be reasonable, because almost all Cu spins are nearly or completely magnetically ordered at 2 K below T_N^{mid} , except for $y=0.10$ in $x=0.10$, $y \geq 0.07$ in $x=0.115$ and $y=0$, and $y \geq 0.07$ in $x=0.13$.
- ²⁹In these pictures, the volume fractions are transformed into the two-dimensional region in the CuO_2 plane. It is noted that, even if the volume fractions are transformed into the three-dimensional region in a sample, the discussion in the text is not changed qualitatively.
- ³⁰Assuming that all the Cu spins in the A_1 regions fluctuate slowly, ξ_{ab} is estimated to be $\sim 30 \text{ \AA}$.
- ³¹K. Yamada, C.H. Lee, K. Kurahashi, J. Wada, S. Wakimoto, S. Ueki, H. Kimura, Y. Endoh, S. Hosoya, G. Shirane, R.J. Birgeneau, M. Greven, M.A. Kastner, and Y.J. Kim, *Phys. Rev. B* **57**, 6165 (1998).
- ³²B. Lake, H.M. Rønnow, N.B. Christensen, G. Aeppli, K. Lefmann, D.F. McMorrow, P. Vorderwisch, P. Smeibidl, N. Mangkorntong, T. Sasagawa, M. Nohara, H. Takagi, and T.E. Mason, *Nature (London)* **415**, 299 (2002).
- ³³H. Matsushita, H. Kimura, M. Fujita, K. Yamada, K. Hirota, and Y. Endoh, *J. Phys. Chem. Solids* **60**, 1071 (1999).
- ³⁴K. Yamada, S. Wakimoto, G. Shirane, C.H. Lee, M.A. Kastner, S. Hosoya, M. Greven, Y. Endoh, and R.J. Birgeneau, *Phys. Rev. Lett.* **75**, 1626 (1995).
- ³⁵H. Kimura, M. Kofu, Y. Matsumoto, and K. Hirota, *Phys. Rev. Lett.* **91**, 067002 (2003).
- ³⁶S. Katano, M. Sato, K. Yamada, T. Suzuki, and T. Fukase, *Phys. Rev. B* **62**, R14677 (2000).
- ³⁷T. Suzuki, T. Goto, K. Chiba, T. Shinoda, T. Fukase, H. Kimura,

- K. Yamada, M. Ohashi, and Y. Yamaguchi, *Phys. Rev. B* **57**, R3229 (1998).
- ³⁸H. Kimura, K. Hirota, H. Matsushita, K. Yamada, Y. Endoh, S.-H. Lee, C.F. Majkrzak, R. Erwin, G. Shirane, M. Greven, Y.S. Lee, M.A. Kastner, and R.J. Birgeneau, *Phys. Rev. B* **59**, 6517 (1999).
- ³⁹M. Hücker, V. Kataev, J. Pommer, J. Haraß, A. Hosni, C. Pflichtsch, R. Gross, and B. Büchner, *Phys. Rev. B* **59**, R725 (1999).
- ⁴⁰O.P. Vajk, P.K. Mang, M. Greven, P.M. Gehring, and J.W. Lynn, *Science* **295**, 1691 (2002).